Current Biology, Vol. 12, 622–631, April 16, 2002, ©2002 Elsevier Science Ltd. All rights reserved. PII S0960-9822(02)00764-9

A Conserved Interaction between β1 Integrin/PAT-3 and Nck-Interacting Kinase/MIG-15 that Mediates Commissural Axon Navigation in *C. elegans*

Patrice Poinat,[1] Adèle De Arcangelis,[1] Satis Sookhareea,[1] Xiaoping Zhu,[2] Edward M. Hedgecock,[2] Michel Labouesse,[1,3] and Elisabeth Georges-Labouesse[1,3]

[1]Institut de Génétique et de Biologie Moléculaire et Cellulaire
CNRS/INSERM/ULP
BP 163
67404 Illkirch
Communauté urbaine de Strasbourg
France

[2]Department of Biology
Johns Hopkins University
Baltimore, Maryland 21218

Summary

Background: Integrins are heterodimeric (αβ) transmembrane receptors for extracellular matrix (ECM) ligands. Through interactions with molecular partners at cell junctions, they provide a connection between the ECM and the cytoskeleton and regulate many aspects of cell behavior. A number of integrin-associated molecules have been identified; however, in many cases, their function and role in the animal remain to be clarified.

Results: We have identified the Nck-interacting kinase (NIK), a member of the STE20/germinal center kinase (GCK) family, as a partner for the β1A integrin cytoplasmic domain. We find that NIK is expressed in the nervous system and other tissues in mouse embryos and colocalizes with actin and β1 integrin in cellular protrusions in transfected cells. To demonstrate the functional significance of this interaction, we used *Caenorhabditis elegans*, since it has only one β (PAT-3) integrin chain, two α (INA-1 and PAT-2) integrin chains, and a well-conserved NIK ortholog (MIG-15). Using three methods, we show that reducing *mig-15* activity results in premature branching of commissures. A significant aggravation of this defect is observed when *mig-15* activity is compromised in a weak *ina-1* background. Neuronal-specific RNA interference against *mig-15* or *pat-3* leads to similar axonal defects, thus showing that both *mig-15* and *pat-3* act cell autonomously in neurons. Finally, we show a genetic interaction between *mig-15*, *ina-1*, and genes that encode Rac GTPases.

Conclusions: Using several models, we provide the first evidence that the kinase NIK and integrins interact in vitro and in vivo. This interaction is required for proper axonal navigation in *C. elegans*.

[3]Correspondence: georges@igbmc.u-strasbg.fr (E.G.-L.), lmichel@igbmc.u-strasbg.fr (M.L.)

Background

Cell interactions with the extracellular matrix are essential for numerous aspects of cell behavior in the organism. In particular, during development, the attachment of cells to their substrate regulates cell motility and cell shape and is required for cell migration or differentiation, tissue organization, and integrity [1, 2]. Integrins are the main receptors that mediate cellular interactions with ECM ligands, such as laminins, collagens, and fibronectin. Genetic analysis has shown that integrins and ECM molecules are required in vertebrates and invertebrates for many aspects of embryogenesis, particularly for epithelial (epidermal attachment, lung development, and morphogenesis of the apical ectodermal ridge) and nervous system development (brain lamination, neuroblast migration, and axon fasciculation) [1, 2]. In some instances, it has allowed us to define which specific ligands or receptors are required in a given tissue [1, 2]. However, while the participation of integrins in signaling pathways is largely recognized as being essential to their function in cultured cells, the mechanisms and functions of integrin signaling in vivo are poorly understood [3, 4]. In cells, signaling by integrins relies on the interactions that they can establish with other molecules and the recruitment of partners at cell junctions [3, 4]. Molecules associated with integrins include cytoskeletal elements, such as talin, filamin, or α-actinin. Indeed, the role of integrins in the organization and dynamics of the cytoskeleton is well documented [5]. Integrins also interact, directly or indirectly, with signaling molecules, like the focal adhesion kinase FAK or the integrin-linked kinase ILK. Genetic analysis has confirmed that a link exists between integrins and these two kinases, in that the phenotype of mouse FAK−/− mutants shares some similarities with the fibronectin mutant phenotype and that, in *Drosophila*, ILK is involved in muscle attachment and wing development like the integrin chain βPS [6, 7]; however, the ILK kinase activity does not seem to be involved in these processes. For a number of other molecules recently identified as integrin α or β chain partners (for recent reviews, see [3, 4]), their relationship with integrins in vivo remains to be analyzed. In a search for molecules that interact with β1 integrin in the embryo, we have found that the kinase NIK, a member of the STE20/GCK family, interacts molecularly with the cytoplasmic domain of integrin β1. Using a genetic approach in the nematode *Caenorhabditis elegans*, we demonstrate that this interaction is required in vivo during commissural axon navigation.

Results

The GCK Serine-Threonine Kinase NIK Interacts with the Cytoplasmic Domain of β1A Integrin

To search for cytoplasmic molecules that interact with the β1 integrin subunit in the mouse embryo, we initiated a yeast two-hybrid screen using, as a bait, the cyto-

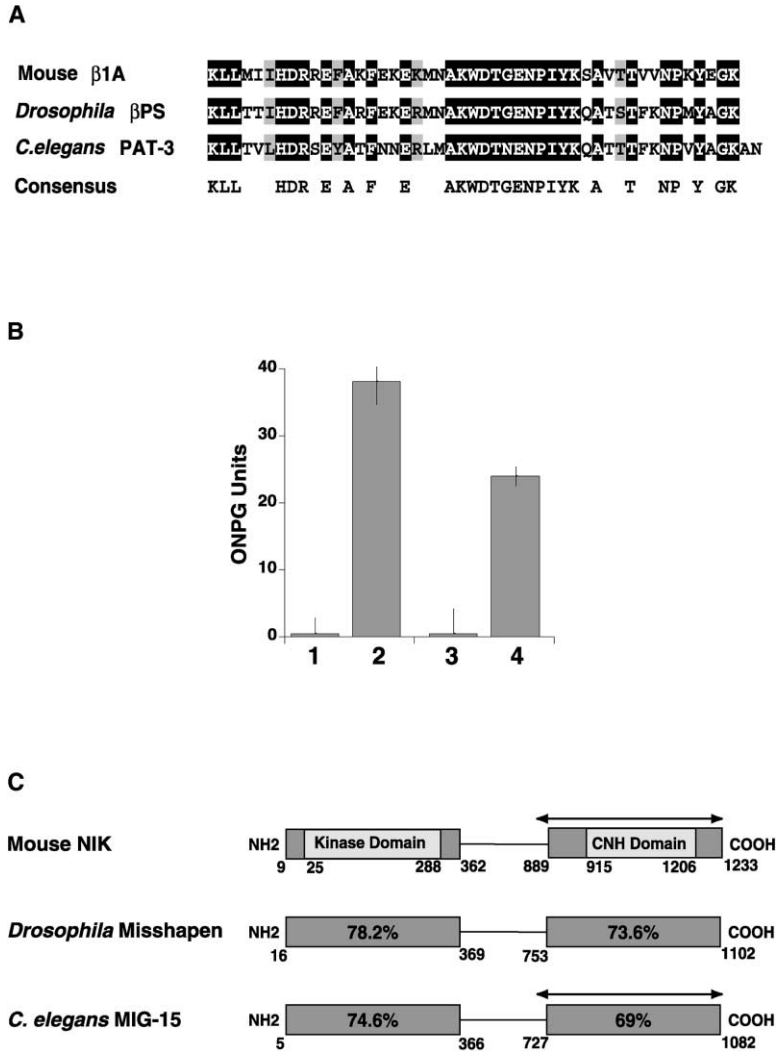

Figure 1. Identification of NIK as a Partner for the β1A Cytoplasmic Domain in a Two-Hybrid Screen

(A) Amino acid sequences of the cytoplasmic domains of mouse β1A (amino acids [aa] 732–778), *Drosophila* βPS (aa 800–846), and *C. elegans* PAT-3 (aa 761–807) integrin chains.

(B) Interaction between LexA-β1A and VP16-NIK (lane 2) and LexA-PAT-3 and VP16-MIG-15 (lane 4). L40 yeast cells carrying the LexA-β1A (lanes 1 and 2) or the LexA-PAT-3 (lanes 3 and 4) were transformed with the VP16 control (lanes 1 and 3), the VP16-NIK (lane 2), or the VP16-MIG-15 plasmids (lane 4). The interaction between the fusion proteins is expressed as ONPG units.

(C) Similarities between NIK, Misshapen, and MIG-15. The three polypeptides are members of the STE20/GCK family, which is characterized by an N-terminal kinase domain and a C-terminal regulatory domain. The 1.9-kb fragment pulled out by the two-hybrid screen corresponded to the C-terminal part of mouse NIK (aa 811–1233, arrow) and a 3′ untranslated segment.

plasmic domain of the β1A subunit, the most broadly expressed β1 isoform. This cytoplasmic domain shows a high degree of conservation between different species, as illustrated for mouse, *Drosophila*, and *C. elegans* in Figure 1A. Three of the clones that we isolated corresponded to the C terminus of the Nck-interacting kinase, NIK. The level of β-galactosidase activity in ONPG assays (Figure 1B, lane 2) suggested that the interaction may be weak, as compared to unrelated control proteins known to interact strongly (data not shown).

NIK, like other GCK family members, is characterized by an N-terminal kinase domain and a C-terminal regulatory region containing binding sites for the Nck adaptor protein and MEKK1 [8–11]. As recently reviewed [10, 11], NIK belongs to the GCK-IV subfamily, which is composed of several members, including orthologs in invertebrates, the Misshapen serine/threonine kinase in *Drosophila*, and the protein encoded by the gene *mig-15* in *C. elegans*, which was identified in unrelated screens for cell migration-defective mutants (X.Z. and E.M.H., unpublished data) [12–14]. Both the N-terminal region containing the kinase domain and the C-terminal regulatory region show a high degree of homology in vertebrates and invertebrates (Figure 1C). In particular, a domain called CNH (citron homology domain), first described in the Rho GTPase effectors citron and citron kinase and thought to regulate the activity of these proteins, is present and is very well conserved in these three NIK orthologs [15]. The fragment (amino acids 811–1233) isolated in our screen corresponds to the C-terminal part of NIK (Figure 1C, arrow) containing the CNH domain.

NIK Interacts with the β1 Cytodomain In Vitro and in Cells

To confirm this interaction, we performed GST pull-down assays in which a bacterially produced GST-β1 (cytoplasmic domain) fusion protein bound to glutathione beads (Figure 2A, lower panel) was incubated with radiolabeled full-length or truncated (amino acids 811–1233) NIK. In both cases, a small fraction of the labeled NIK was found to be retained by the GST-β1 beads and not by the GST beads (Figure 2A, top and middle panels). The low percentage of bound NIK may reflect the fact that the interaction is weak, as mentioned above (Figure 1B). To see whether this interaction can also take place

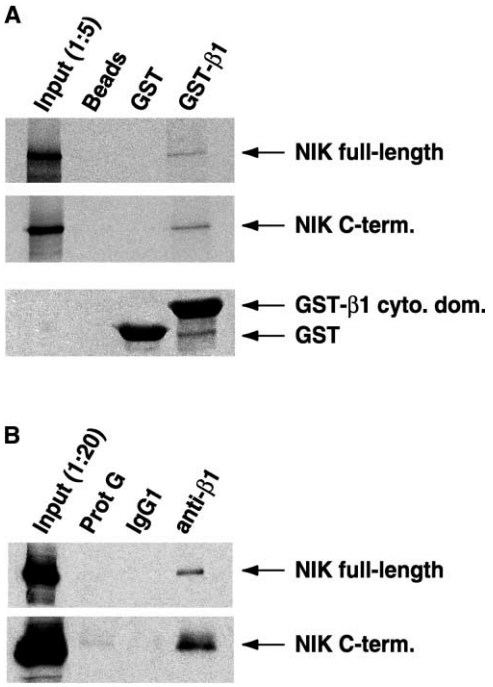

Figure 2. Association of NIK and β1 Integrin In Vitro and in Cells

(A) Equimolar amounts of GST or GST-β1 cytoplasmic domain (lower panel, GST and GST-β1 cyto. Dom.) were incubated with radiolabeled full-length NIK (upper panel) or the NIK C terminus (NIK C-term. Domain, spanning the 811–1233 aa region, middle panel). Bound NIK was visualized by autoradiography. Input corresponds to one-fifth of the total radiolabeled NIK.

(B) HeLa cells were transfected with myc-tagged full-length NIK (upper panel) or the NIK C terminus (lower panel, NIK C-term.). Cells were recovered by EDTA treatment and were either incubated with PBS (Prot G, second lane), control mouse IgG1 (IgG1, third lane), or with the mouse monoclonal antibody TS2/16.2.1 against human β1 integrin (anti-β1, fourth lane). The first lane corresponds to a 1:20 part of the supernatant. The myc-tagged NIK was detected using a polyclonal anti-myc antibody.

in cells, HeLa or COS cells transfected with myc-tagged full-length or truncated NIK cDNAs were incubated with an antibody against β1 after plating on a laminin substrate. Both with the full-length NIK and the C-terminal NIK-transfected cells, a fraction of the myc-tagged NIK could be found in the immunoprecipitates with the anti-β1, as shown in Figure 2B for HeLa cells.

NIK Colocalizes with Actin and β1 Integrin in the Tips of Cellular Protrusions

To look at the subcellular localization of NIK, the full-length myc-tagged NIK cDNA was transfected into mouse NIH 3T3 fibroblasts. Stably transfected cells were plated either on polylysine-, fibronectin-, or laminin-coated coverslips and were analyzed at different time points after plating. Strikingly, a very distinct signal was observed at early time points after seeding (Figures 3A and 3D), but not after overnight cultures (data not shown). This was mostly visible in cells cultured on laminin substrates after 2 hr (Figures 3A and 3D) or on polylysine coverslips after 6 hr (data not shown). Cells that showed the most typical localization of NIK were often stellate shaped and extended several thick processes (Figures 3A and 3D). In those cells, in addition to a general intracellular signal, a strong signal was visible at the tips of filopodia-like cellular protrusions (Figures 3A and 3D and insets, arrows). Localized signals were also visible in lamellipodia (Figure 3A, arrowhead). Those two sites of the highest NIK concentration were also very intensely stained for actin (Figures 3B and 3C and insets). The antibody against β1 integrin also revealed an enrichment of this integrin in the same tips (Figures 3E and 3F and insets). Importantly, the sites of colocalization between β1 and NIK do not coincide with the main other sites where β1 is present, such as focal adhesions seen in Figure 3E. The dynamic cellular localization of NIK and its colocalization with actin and β1 integrin suggest that NIK may interact with integrins during cell adhesion/spreading or motility.

NIK Is Highly Expressed in the Nervous System of the Mouse Embryo

To gain an insight into NIK function, we characterized its expression pattern in the mouse embryo. Both a 3′ fragment and a central fragment (see the Supplementary Material available with this article online) were used as probes for in situ hybridization of mouse embryos and yielded very similar results. NIK was found to be widely expressed at all stages examined (embryonic days E10.5, E12.5, and E14.5), the level of expression being particularly strong in the nervous system (Figure 4A). In the central nervous system, a signal was found in the cortex, striatum, spinal cord, and retina (Figure 4). Dorsal root ganglia were also strongly labeled (Figure 4C). Expression in the cortex was somewhat reminiscent of that observed for β1 and α6 integrins [16]. This expression pattern is consistent with developmental functions, particularly in the nervous system.

Interactions between PAT-3 and MIG-15 in *C. elegans*

In order to investigate the potential biological significance of the interaction between β1 integrin and NIK, we turned to *C. elegans*, since its anatomical and genetic simplicity could help to determine the biological processes requiring this interaction. As already mentioned, there is a unique locus corresponding to a NIK ortholog in the *C. elegans* genome called *mig-15*. In addition, two α (PAT-2 and INA-1) and one β (PAT-3) integrin chains have been identified in *C. elegans* by mutations [17–20]. INA-1, which can bind PAT-3, is more closely related to the α3, α6, and α7 subgroup of vertebrate integrin chains [18, 19]. INA-1/PAT-3 may thus correspond to a laminin binding integrin, while PAT-2/PAT-3 would be the RGD binding integrin [19]. First, we tested if PAT-3 can also interact with MIG-15 in vitro. As shown in Figure 1B (lane 4), using a two-hybrid ONPG assay, we could detect an interaction between the cytoplasmic domain of PAT-3 and the C-terminal part of MIG-15, which was in the same order of magnitude as that between β1A integrin and NIK. We conclude that the interaction between the two proteins has been evolutionarily conserved.

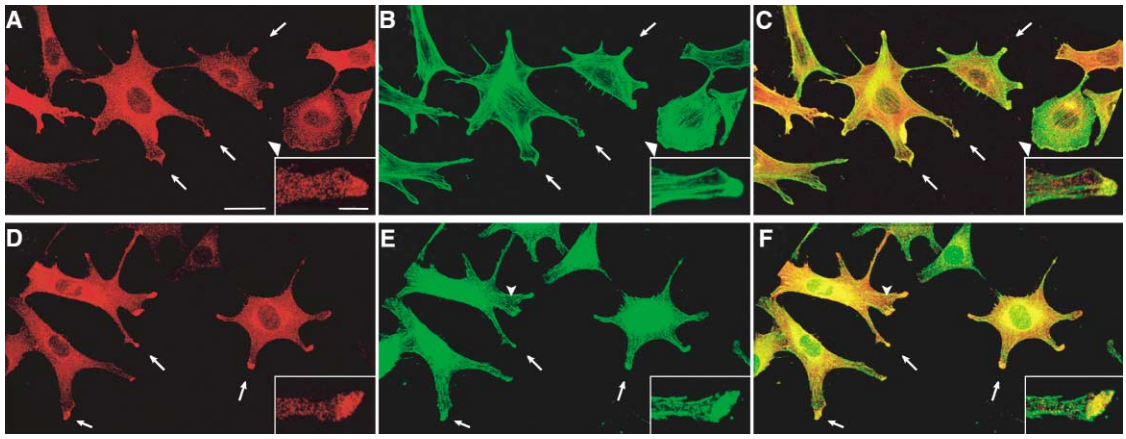

Figure 3. Colocalization of NIK with Actin and β1 Integrin in Cellular Protrusions

(A and D) 3T3 cells, 2 hr after plating on laminin, expressing the myc-NIK fusion protein immunolabeled for the myc tag by the 9E10 monoclonal antibody. The signal is mainly localized at the tips of cellular processes (arrows) and at the edge of lamellipodia (large arrowhead in [A]).

(B) Actin (phalloidin) staining of the cells showed in (A).

(C) A merged picture of (A) and (B) showing colocalization of myc-NIK and actin in tips and lamellipodia.

(E) β1 integrin immunolabeling of the cells showed in (D). β1 integrin is present in focal adhesions (arrowhead) and in the tips of the cell protrusions (arrows).

(F) A merged picture of (D) and (E) showing colocalization of myc-NIK and β1 integrin in the tips. The insets in each panel correspond to higher magnification. The scale bar represents 30 μm in (A)–(F) and 5 μm in the insets in (A)–(F).

NIK and Integrins Are Important for Axon Navigation in *C. elegans*

The availability of integrin mutants in *C. elegans* allowed us to test whether NIK and integrins interact genetically. Weak *ina-1* mutations cause cell migration and axon defasciculation defects, and a weak motility defect, but are compatible with life, while the presumptive null mutation *ina-1(gm86)* results in larval lethality, presumably due to abnormal head morphogenesis coupled with more severe axonal defects [18]. Mutations inactivating *pat-2* and *pat-3* cause muscle attachment defects and incomplete elongation of the embryo, resulting in embryonic lethality [17, 20]. As mentioned above, *mig-15* mutations cause some cell migration defects that are in part distinct from those observed in *ina-1* mutants (X.Z. and E.M.H., unpublished data). To initiate a genetic analysis of *mig-15* and determine if it could be involved in the same process as PAT-2/PAT-3 or INA-1/PAT-3, we first used an RNA interference strategy (RNAi) to inhibit *mig-15* activity [21]. The main advantage of RNAi is that it is extremely rapid and can result in a nearly complete loss-of-function phenotype, particularly for genes acting in embryos; its disadvantage is that genes acting during postembryonic development, particularly in neurons, tend to be less strongly inhibited [22].

Injecting *mig-15* dsRNA into a wild-type strain resulted in slightly reduced fertility and motility (data not shown), but did not produce a phenotype similar to the muscle attachment defects described for *pat-3* or *pat-2* mutations. The weak motility defects raised the possibility that *mig-15* could be involved in the same process as *ina-1*. To test if this was the case, we repeated the

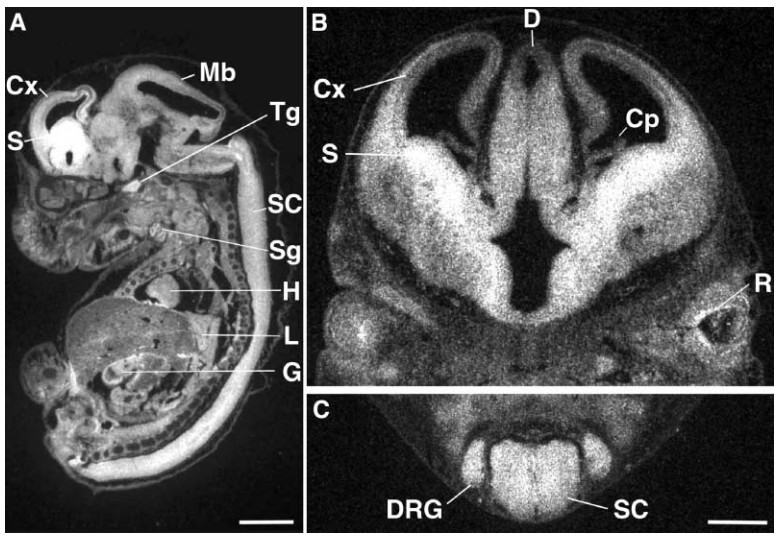

Figure 4. Expression of NIK in the Mouse Embryo

(A) A sagittal section of an E14.5 mouse embryo, showing expression in several tissues and the brain and spinal cord.

(B) A coronal section of an E12.5 embryo at a higher magnification. Note the very strong signal in the striatum and the moderate signal in the layers of the cortex (ventricular zone and cortical plate) and in the neural retina.

(C) A very strong signal at higher magnification in a transverse section through spinal cord and dorsal root ganglia.

Abbreviations: Cx, cortex; Cp, choroid plexus; D, diencephalon (thalamus); DRG, dorsal root ganglia; G, gut; H, heart; L, lung; Mb, midbrain; R, retina; S, striatum (ganglionic eminence); SC, spinal cord; Sg, submandibular gland; Tg, trigeminal (V) ganglion. The scale bar represents 1.5 mm in (A) and 0.5 mm in (B) and (C).

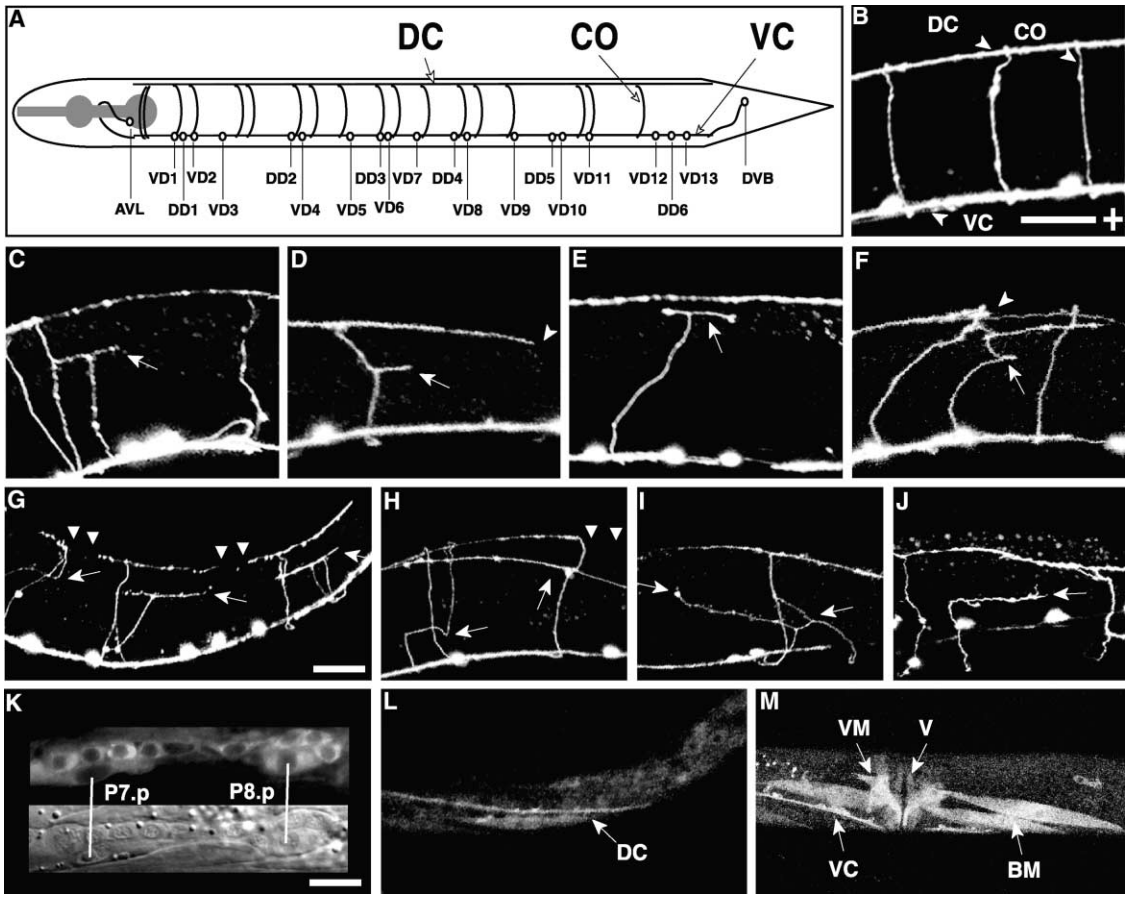

Figure 5. Similar Axon Navigation Defects in *ina-1*- and *mig-15*-Deficient Animals

(A) A schematic diagram of *C. elegans* GABAergic neurons: the name of all GABAergic neurons are indicated below the cell bodies (white circles); DC, dorsal cord; CO, commissure; VC, ventral cord. Anterior is oriented toward the left, and dorsal is oriented upward. Note that most commissures are on the right side of the animal (curved lines pointing to the tail), while two in the head are on the left side (curved lines pointing to the head).

(B) GFP autofluorescence of a wild-type control animal carrying the *unc-47::gfp* transgene expressed in all GABAergic neurons.

(C–J) Commissures from a (C) *mig-15(RNAi)* animal, a (D) *mig-15(rh148)* mutant, an (E) *ina-1(gm144)* mutant, an (F) *ina-1(gm119); mig-15(rh148)* double mutant, an (G) *ina-1(gm144); mig-15(RNAi)* mutant, an (H and I) animal carrying a transgene expressing *mig-15* dsRNA and *pat-3* dsRNA, respectively, under the control of the *unc-25* GABAergic promoter, and an (J) *ina-1(gm144)* mutant after stable *mig-15* RNAi under the control of the *unc-25* promoter. All animals carry the *unc-47::gfp* construct. Note that most animals have meandering commissures and/or prematurely branched commissures (arrows) that generally lead to a disruption of the dorsal cord (arrowheads), and that the defects are significantly more severe when animals are defective for both *ina-1* and *mig-15*.

(K) Upper panel, expression of *mig15::gfp* in neurons of an L2 larva in the area of P7.p–P8.p cells (ventral side is up); lower panel, DIC (differential interference contrast) picture of the same animal (only the ventral cord is shown).

(L) Expression of *mig-15::gfp* in the dorsal cord (DC) in an L3 animal.

(M) Expression of *mig-15::gfp* in the ventral cord (VC), body wall (BM), vulval (VM) muscles, and vulva (V) of a young adult. In panels (H)–(M), the animal appears to be twisted because of the dominant marker *rol-6(su1006)* used as a cotransformation marker. The scale bar represents 30 μm in (B)–(L) and (M) and 6 μm in (K).

RNAi experiments in a strain expressing a GFP marker that allowed us to visualize the positions and axonal trajectories of the GABAergic motoneurons, in which *ina-1* is known to be required [18, 23]. We used an *unc-47::gfp* construct, which is expressed in these neurons [24, 25]. Normally, each axonal projection of the GABAergic D-type neurons, which are located in the ventral body region, exits the ventral cord (major ventral axonal bundle) to form a circumferential commissure that reaches the dorsal cord, generally on the right side of the animal, and branches both anteriorly and posteriorly as short projections in the dorsal cord (Figure 5A). The 6 DD neurons, which are generated during embryogenesis, extend their commissures in the embryo, while the 13 VD neurons, which are born during the late L1 larval stage, do so during the L2 larval stage. In the *unc-47::gfp* background, all GABAergic axons form a tight bundle in the ventral and dorsal cords (Figures 5A and 5B), and each commissure can be individually visualized (Figure 5B).

Mutations in *ina-1* have been reported to cause defasciculation of the ventral and dorsal cords, occasional commissural outgrowth on the left side of the animal, and, more rarely, failure to reach the dorsal cord [18, 23]. We could indeed observe these defects after intro-

ducing the *unc-47::gfp* marker into the weak mutants *ina-1(gm119)* and *ina-1(gm144)* (Figure 5E). When *mig-15* dsRNA was injected into the *unc-47::gfp* background, we observed a similar range of defects. In particular, some commissures meandered to reach the ventral cord or, less frequently, branched prematurely in the dorsal part of the animals where muscles are found before reaching the dorsal cord (Figure 5C and the Supplementary Material). These defects suggest a role for *mig-15* in axonal navigation, as reported for *Drosophila misshapen* [9, 14].

To examine if *mig-15* acts in the same pathway as *ina-1/pat-3*, we reasoned that inducing RNAi against *mig-15* in a weak *ina-1* mutant background should significantly increase the penetrance of axonal defects, while it should not increase the penetrance of defects observed in *ina-1* null mutants. When we introduced *mig-15* dsRNA into *ina-1(gm119)* and *ina-1(gm144)* backgrounds (Figure 5E), we observed that the severity of the commissural defects (Figure 5G) and their penetrance (Figure 6A and data not shown) were significantly increased. In contrast, injecting *mig-15* dsRNA in mothers heterozygous for the null allele *ina-1(gm86)* did not increase the severity of commissural defects in *ina-1(gm86)*-arrested L1 larvae, which, on their own, had essentially normal commissures (in both cases, 5.4 ± 0.7 commissures per animal were normal). The absence of strong defects in *ina-1(gm86)* mutants suggests that *ina-1* is not essential for DD commissure navigation in embryos.

To verify the genetic interaction described above, we took advantage of the weak *mig-15(rh148)* allele (X.Z. and E.M.H., unpublished data), expecting that it should display a commissural defect on its own and that it should genetically interact with a weak *ina-1* allele. Homozygous *mig-15(rh148)* animals containing the *unc-47::gfp* construct displayed the same type of commissural defects (Figures 5D and 6B) as those observed after RNAi against *mig-15*, but their frequency was higher (34% abnormal commissures in *mig-15(rh148)* animals versus 13% in *mig-15(RNAi)* animals, Figures 5D and 6B). Furthermore, in *ina-1(gm119); mig-15(rh148)* double mutants, we observed that most commissures (85%) had abnormal trajectories (Figures 5F and 6B). Interestingly, the relative proportion of commissures that meandered versus commissures that stopped prematurely with a lateral projection was almost inverted in single compared to double mutants. In *ina-1(gm119)* and *mig-15(rh148)* mutants, 60%–70% abnormal commissures meandered and 20%–30% extended a premature lateral projection; in contrast, in double mutants, 40% abnormal commissures meandered and 50% stopped prematurely with an extension. This inversion could be interpreted as an increase in the severity of the phenotype.

Thus, we conclude that *ina-1* and *mig-15* interact genetically, at least during the process of commissure outgrowth and navigation. In addition, we suggest that this interaction is particularly important for the decision to form a lateral projection at the appropriate position.

Integrins and NIK Function in Neurons

Commissural axons that project from the ventral to the dorsal nerve cord navigate between the muscle and the epidermis and have to circumvent obstacles (muscles or lateral nerve cords), which implies a constant reorganization of the growth cone in contact with the basement membrane covering the epidermis and muscle surfaces [25]. Several mechanisms could account for the neuronal defects observed in *mig-15*-defective animals. The first possibility would be that MIG-15 and INA-1/PAT-3 integrin interact and are cell autonomously required in neuronal cells. Another possibility would be that MIG-15 acts in the epidermis or muscles; for instance, it could somehow modify the assembly of the basement membrane and act in a non-cell-autonomous fashion to affect axon extension. We first characterized *mig-15* expression by following the expression of a full-length *mig-15::gfp* reporter construct that partially rescues *mig-15(rh148)* (Figure 6B). At the time of axonal outgrowth during larval development and in adults, we could detect GFP expression in the ventral and dorsal nerve cords (Figures 5K–5M), in the body wall muscles (Figure 5M), and weakly in the epidermis as well as in other tissues/organs (i.e., pharynx) (data not shown), an expression pattern compatible with both interpretations.

To distinguish between a cell-autonomous or a non-cell-autonomous function, we induced stable RNAi [26] using tissue-specific promoters derived from the *unc-25* (GABAergic neuron-specific), the *unc-54* (body wall muscle-specific), and the *lin-26* (epidermal-specific) loci. These promoters were used to drive the expression of either *mig-15* sense or antisense RNA strands, or the expression of both, into the *unc-47::gfp* background. As *pat-3* mutants are not viable, using this approach, we could also directly assess if PAT-3 was indeed required for commissural axon extension, as expected if it is the INA-1 dimerization partner. In the case of *mig-15*, typical neuronal navigation defects such as the ones described above were seen at a significant ratio only in animals in which the RNAi effect was targeted to neurons (Figures 5H and 6A). Similarly, neuronal navigation defects were seen when RNAi against *pat-3* was targeted to neurons (Figure 5I). Since *unc-25*-induced RNAi against *pat-3* did not lead to embryonic lethality (Pat phenotype) nor to any partial muscle paralysis, we conclude that *pat-3* dsRNA produced in neurons did not affect other cell types. Only mild phenotypes were seen when sense or antisense strands alone were expressed, and no defects were seen in transgenic animals carrying a vector with the *unc-25* promoter alone (Figure 6A). Again, the effects were significantly more severe when the construct driving both sense and antisense *mig-15* RNAs under the control of the *unc*-25 promoter were introduced in the *ina-1(gm144)* background (Figures 5J and 6A). These results strongly suggest that GABAergic commissural axon extension requires cell autonomously INA-1/PAT-3 and MIG-15.

Having established that *mig-15* and *ina-1* interact and that both act in neurons, we asked whether MIG-15 works downstream or upstream of the INA-1/PAT-3 integrin, anticipating that, in the former case, it might be possible to rescue *ina-1* by overexpressing MIG-15. We used a heat shock promoter to drive the expression of the entire *mig-15*-coding region with all its introns, rather than a specific cDNA, because there are several MIG-15 isoforms (data not shown) for which possible tissue

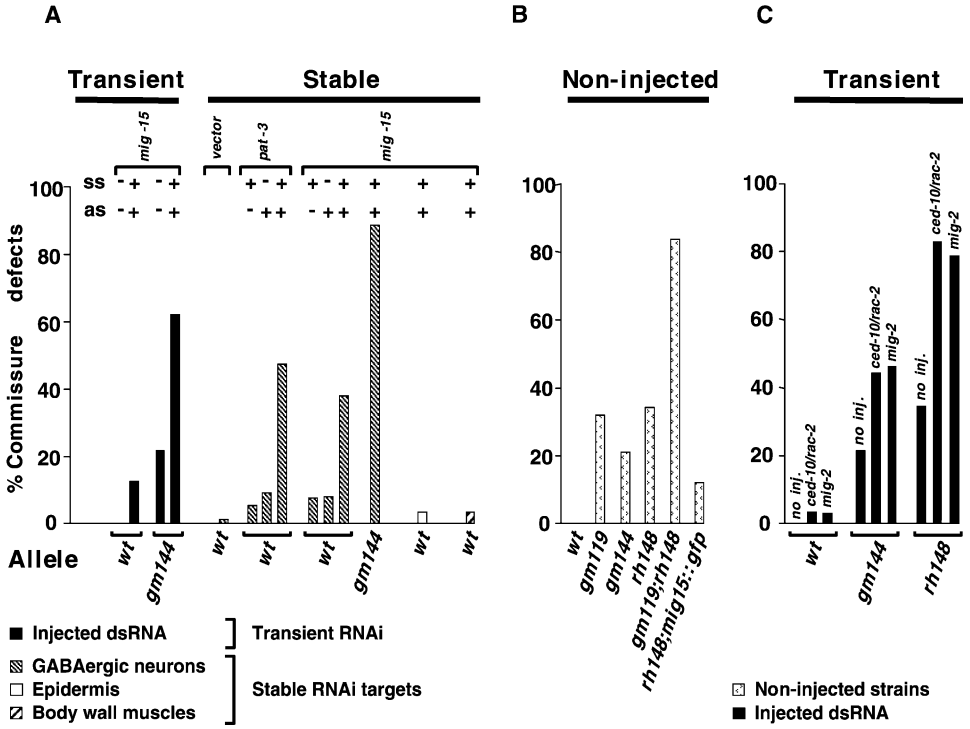

Figure 6. Quantification of Commissural Navigation Defects in Animals Deficient for INA-1, MIG-15, and Rac GTPases

The bars show the percentage of abnormal commissures observed in at least 40 animals.

(A) Transient RNAi (injection) or stable RNAi targeting GABAergic neurons, the epidermis, or body wall muscles, using the *unc-25*, *lin-26*, or *unc-54* promoters, respectively, to drive sense (ss) or antisense (as) strand expression was induced in wild-type (wt) or *ina-1(gm144)* mutant animals carrying the *unc-47::gfp* construct. The effect of stable RNAi was scored in two independent transgenic lines; both lines showed very similar defects, and the result for only one is shown. The average number of abnormal commissures per animal was: wild-type control, 0; *mig-15(RNAi)*, 1.9 ± 1.4; *ina-1(gm144)*, 3.4 ± 1.3; *ina-1(gm144); mig-15(RNAi)*, 8.7 ± 1.6; stable neuronal RNAi against *mig-15*, 5.9 ± 1.5; stable neuronal RNAi against *mig-15* in *ina-1(gm144)*, 13.1 ± 1.3 (in some experimental conditions, fewer commissures than normal could be seen). Note that both by counting the total (A) or the average number of commissures per animal, RNAi against *mig-15* led to a marked increase of the commissural defects compared to what is observed in *ina-1(gm144)* alone (similar synergistic effects were also observed after transient RNAi against *mig-15* in the *ina-1(gm119)* mutant background, data not shown).

(B) *ina-1(gm119)*, *mig-15(rh148)*, and double mutant animals carrying the *unc-47::gfp* construct. The average number of abnormal commissures per animal was: control animals, 0; *ina-1(gm119)*, 5.6 ± 2.6; *ina-1(gm144)* mutants, 3.4 ± 1.3; *mig-15(rh148)* mutants, 6.1 ± 2.5; *ina-1(gm119); mig-15(rh148)* double mutants, 13.9 ± 2.1; *mig-15(rh148)* mutants with the *mig-15::gfp* construct, 1.7 ± 1.2. Note that commissural defects were significantly ($p < 10^{-6}$) more severe in double mutant animals, while expression of the *mig-15::gfp* transgene (see Figures 5K–5M) in *mig-15(rh148)* mutants significantly restored normal outgrowth ($p < 10^{-5}$).

(C) Transient RNAi against *rac-2* (affecting both *ced-10* and *rac-2* expression, see the Supplementary Material) or *mig-2* was performed in wild-type (wt), *ina-1(gm144)*, or *mig-15(rh148)* animals carrying the *unc-47::gfp* construct. The average number of abnormal commissures per animal was: wild-type, 0; *rac-2(RNAi)*, 0.6 ± 0.6; *mig-2(RNAi)*, 0.6 ± 0.7; *ina-1(gm144)*, 3.4 ± 1.3; *ina-1(gm144); rac-2(RNAi)*, 7.3 ± 2.9; *ina-1(gm144); mig-2(RNAi)*, 7.2 ± 2.0; *mig-15(rh148)*, 6.1 ± 2.5; *mig-15(rh148); rac-2(RNAi)*, 11.3 ± 1.9; *mig-15(rh148); mig-2(RNAi)*, 11.1 ± 1.7. Note the significant increase ($p < 10^{-6}$) of commissural defects in injected mutant animals compared to what is observed in noninjected (no inj.) mutants or wild-type injected animals.

specificity is unknown. By doing so, we could significantly rescue the commissural defects of *mig-15(rh148)* animals upon heat shock induction, indicating that the transgene is functional (data not shown). However, when we performed the same experiments in the *ina-1(gm144)* or *ina-1(gm119)* backgrounds, we did not observe any rescue. The proportion of abnormal commissures was even almost doubled in *ina-1(gm144)* mutants (data not shown). This aggravation may be related to the nature of the *ina-1(gm144)* allele that alters a residue located just upstream of the transmembrane domain and behaves differently from other *ina-1* alleles for some aspects of the *ina-1* mutant phenotype [18]. The lack of consistent behavior between both alleles does not allow us to conclude whether *mig-15* acts downstream or upstream of *ina-1*.

ina-1 and *mig-15* Genetically Interact with Rac GTPases

In a first attempt to determine the pathway involving integrins and NIK in axon outgrowth and navigation, we first tested members of the Rho/Rac/Cdc42 family, which are known to play an important role in actin dynamics [5, 27]. In *C. elegans*, it was recently shown that mutations in the Rac homologs *ced-10* (also known as *rac-1*) and *mig-2*, or RNAi against *rac-2*, result in mild D-type neurons' commissural defects on their own and in severe defects when two distinct Racs are defective [28]. We found that RNAi against the highly homologous *ced-10* and *rac-2*, or against *mig-2* in *mig-15* or *ina-1* mutants, approximately doubled the percentage of affected commissures when injected in animals carrying either *ina-1(gm144)* or *mig-15(rh148)* (Figure 6C), while

they produced essentially no effect in a wild-type background. Since the effects were more than additive, it suggests that there is a genetic interaction between Rac GTPases and integrins or NIK.

Discussion

Our studies have revealed a molecular interaction between the cytoplasmic domain of the β1 integrin subunit and the C terminus of the serine-threonine kinase NIK. Several lines of evidence indicate that this interaction is required in cell/growth cone motility. First, NIK is expressed at high levels in the nervous system. Second, at the cellular level, NIK is colocalized with actin and β1 integrin in cells at early stages of spreading or motility, in the tips of filopodial-like extensions, which may resemble growth cone extensions. Finally, there is a genetic interaction in *C. elegans* between *mig-15* and the integrin *ina-1* in neuronal cells that is required for proper axon navigation.

Neuronal navigation relies on guidance molecules and cell surface receptors that signal through a number of pathways to regulate cytoskeletal organization and membrane dynamics [27]. To understand the function of MIG-15 and INA-1, it is necessary to recall how GABAergic neurons extend their commissures [29]. Commissural axons grow circumferentially at a constant rate until they meet obstacles (lateral axons or muscles), at which point the growth cone stalls to find its way around the obstacle [25]. As discussed by Knobel et al., stalling may represent a lag imposed by the signal transduction machinery to reorganize surface molecules or the cytoskeleton [25].

The commissural defects that we observed in *ina-1*-, *pat-3*-, and *mig-15*-deficient larvae correspond to two main categories. In single mutants, a majority of commissures meandered instead of following a direct trajectory toward the dorsal cord, which could be interpreted as a partial failure in maintaining a strict navigation toward the guidance cues. In double mutants, the majority of commissures stopped prematurely and extended laterally in both directions, as they normally do when they reach the dorsal cord. This defect could originate from problems in passing beyond obstacles, as indeed most axons branching prematurely did so where muscles are found (Figure 5 and data not shown). This suggests that INA-1/PAT-3 and MIG-15 are required to stabilize the growth cone along a precise direction and are required for the cell to respond appropriately when signaling in the growth cone must change. They may act by controlling cytoskeletal organization, since integrins are known to affect actin dynamics [5, 30] and since a link between GCK kinases and the cytoskeleton has been suggested before [11].

As previously discussed by Baum et al. for *ina-1* [18], and as observed in *Drosophila* for PS integrins [31] and *misshapen* (*msn*; the *mig-15* homolog in fly) [9, 14], our data suggest that integrins and NIK are not essential for commissure extension per se. However, it cannot be ruled out that complete loss of function in both *ina-1*/*pat-3* and *mig-15* would lead to more drastic outgrowth phenotypes. We did not observe defects that could correspond to an improper response to a stop signal, as described for *msn*, which appears to be required in photoreceptor axons for proper targeting and response to stop signals [9]. These apparent differences may reflect differences in cell types (motoneuron versus photoreceptor) or between organisms.

As we have not been able to determine whether *mig-15* acts downstream or upstream of *ina-1*, we can imagine two opposite models to account for the biochemical role of INA-1/PAT-3 and MIG-15 in growth cone motility. In a model in which *mig-15* would act upstream of *ina-1*, one could imagine that, in response to changes in actin dynamics or GTPase activity initially triggered by some other membrane receptors, MIG-15 interacts with PAT-3 to modulate integrin engagement. It could achieve this effect by phosphorylating the integrin, which contains a few conserved serine and threonine residues, or proteins that are associated to it. This phosphorylation event could be part of the integrin activation process whose mechanisms remain largely unknown. Alternatively, if *mig-15* acts downstream of *ina-1*, the integrin could, in response to changes in the ECM microenvironment, interact with MIG-15, which would in turn interact with or phosphorylate downstream targets, resulting in changes in growth cone motility.

In *C. elegans*, molecules that are required for commissural outgrowth or navigation include UNC-6/netrin and its receptor UNC-5 [29, 32]; laminin (EPI-1) [23], which is a potential ligand of INA-1/PAT-3; the actin binding protein UNC-115 [33]; the guanine nucleotide exchange factor Trio (UNC-73) [23, 34]; and three Rac GTPases (CED-10, RAC-2, and MIG-2) [28]. Our data suggest a functional link between Rac GTPases, NIK, and integrins. Since multiple pathways converge on Racs (for instance, see reference [28]), the precise relationship between Racs and these molecules in axonal outgrowth remains to be clarified.

There is indirect evidence to suggest that integrins and NIK proteins could interact in other cell types or tissues. For instance, both *msn* and the fly βPS *myospheroid* mutants display defects in the process of dorsal closure [1, 13, 35]. Moreover, an interaction between integrins and NIK may explain the similarities recently reported between the phenotypes of NIK−/− and fibronectin or integrin α5−/− mutant mouse embryos [36]. This suggests that, during mesoderm formation, too, NIK and integrins might participate in the same pathway. There are more than ten integrins that contain the β1 subunit in vertebrates, and it will be interesting to define whether only a specific set of those integrins interacts with NIK. It is quite possible that NIK, like integrins, act in several pathways by different mechanisms. For example, the function of Msn during dorsal closure in *Drosophila* seems to require the Jun kinase pathway, but not Nck (Dock) [14], while there is one report that it may act through Dock and not through the Jun kinase pathway during retinal axon targeting [9]. Further genetic analyses combining invertebrate and vertebrate models should help to clarify the relationship between NIK and integrins and to further dissect the signaling pathways in which they are involved.

Experimental Procedures

A more detailed description of the methods can be found in the Supplementary Material.

Constructs for Two-Hybrid Experiments

Fragments corresponding to the cytoplasmic domains of mouse β1A or *C. elegans* PAT-3 integrins were cloned into the pLex9-3H plasmid in frame with LexA [37]. A E9.5–E12.5 mouse embryo cDNA library in the pASV3 plasmid, in frame with the VP16-coding sequence (J.M. Garnier, IGBMC) was used for the screen. A partial *mig-15* cDNA corresponding to the NIK fragment isolated in the two-hybrid screen was obtained by RT-PCR and was cloned into the pASV3 plasmid in frame with the VP16-coding sequence. Yeast manipulations were carried out in the L40 strain (*MATa, trp1, his3, leu2, ade2, LYS2::(LexAop)$_4$-HIS3, URA3::(LexAop)$_8$-LacZ*) as described [37].

GST Pull-Down and Coimmunoprecipitation Experiments, Cellular Localization of NIK

The cytoplasmic domain of the β1A integrin was cloned in frame with the GST ORF into the pGex4T1 vector (Amersham Pharmacia Biotech). The 3′ part of NIK (nucleotides 2431–3702), flanked by a hemagglutinin (HA) tag, was cloned into the pET15b vector (Novagen). NIK full-length cDNA was cloned in frame at its N terminus with a 6× myc epitope tag, downstream of the cytomegalovirus promoter (gift of plasmid from P. Blader, IGBMC). A cotranscription/translation reaction in a rabbit reticulocyte lysate system (Promega) was performed to generate [^{35}S]methionine polypeptides. Coimmunoprecipitation of NIK and β1 integrin was performed using HeLa or COS cells transfected with the myc-tagged full-length or truncated NIK cDNA as described [38]. For cellular localization of NIK, 3T3 fibroblasts stably transfected with the myc-NIK full-length plasmid were used.

C. elegans Strains and Manipulations

Strain EG1285, *oxIs12* [*unc-47*::GFP; *lin-15(+)*] *lin-15(n765ts)* LGX, expressing the green fluorescent protein (GFP) in GABAergic neurons [24], and *ina-1* mutants were obtained from E. Jorgensen and the *Caenorhabditis* Genetic Centre (CGC), respectively. The identification of *mig-15(rh148)* will be reported elsewhere (X.Z. and E.H., unpublished data). Transient RNAi was performed as described elsewhere [21]. To obtain stable RNAi effects, we generated transgenic animals expressing a *mig-15* or a *pat-3* cDNA fragment under tissue-specific promoters. *mig-15* and *pat-3* fragments were subcloned in both orientations in the pSC325 plasmid containing the *unc-25* promoter and terminator [39]. The *mig-15* fragment was also cloned into the plasmid pML450, containing part of the *lin-26* epidermal promoter and the *unc-54* terminator (F. Landmann and M.L., unpublished data), or into the plasmid pPD30.38, containing the *unc-54* muscle promoter and terminator [39]. To generate a rescuing *mig-15::gfp* construct, two fragments were coinjected to generate stable transgenic animals: a 3.8-kb fragment corresponding to part of the *mig-15* gene up to its last codon obtained after PCR amplification and cloning in frame into the GFP vector pPD95.75 (gift from A. Fire) [40]; and a 13-kb fragment corresponding to the rest of the gene and its putative promoter (overlap of 2 kb with the previous fragment) obtained after PCR amplification. To overexpress *mig-15*, a PCR fragment corresponding to the *mig-15* gene starting 20 nucleotides prior to the *mig-15* initiation codon and finishing immediately after the stop codon was cloned downstream of the heat shock-responsive promoter *hsp16-2* (vector pPD49.78) [41]. Transgenic animals were obtained by coinjection either with the plasmid pRF4, which confers a dominant roller phenotype, or with the *myo-2::gfp* plasmid pPD118.33 expressed in the pharynx (gifts from A. Fire). For heat shock experiments, transgenic L1 larvae were subjected to a single heat shock (15 min at 30°C or 60 min at 32°C), and commissural defects were observed in young adults raised at 20°C. Animals from two independent lines were examined in all cases.

Supplementary Material

Supplementary Material including more detailed Experimental Procedures and additional data on dorsal cord disruptions and fasciculation defects is available at http://images.cellpress.com/supmat/supmatin.htm.

Acknowledgments

We thank M. Boeglin, D. Hentsch, N. Messaddeq, and J.L. Vonesch for assistance in confocal microscopy and image analysis. We are grateful to P. Blader, A. Fire, Y. Jin, S. Johannson, E. Jorgensen, F. Landmann, and the CGC for the kind gift of strains and reagents and to H. Boeuf, G. Gradwohl, R. Losson, and Y. Jin for helpful discussions. This work was supported by institutional funds from the Centre National de la Recherche Scientifique (CNRS), the Institut National de la Santé et de la Recherche Médicale (INSERM), and the Hôpitaux Universitaires de Strasbourg (HUS) and grants to E.G.-L. and M.L. from the Association pour la Recherche sur le Cancer (ARC) and the Ministère de la Recherche ACI "Biologie du développement et physiologie intégrative". P.P. was supported by fellowships from the Ministère de la Recherche and the ARC.

Received: May 16, 2001
Revised: January 3, 2002
Accepted: January 11, 2002
Published: April 16, 2002

References

1. Brown, N.H. (2000). Cell-cell adhesion via the ECM: integrin genetics in fly and worm. Matrix Biol. *19*, 191–201.
2. De Arcangelis, A., and Georges-Labouesse, E. (2000). Integrin and ECM functions: roles in vertebrate development. Trends Genet. *16*, 389–395.
3. Liu, S., Calderwood, D.A., and Ginsberg, M.H. (2000). Integrin cytoplasmic domain-binding proteins. J. Cell Sci. *113*, 3563–3571.
4. van der Flier, A., and Sonnenberg, A. (2001). Function and interactions of integrins. Cell Tissue Res. *305*, 285–298.
5. Schoenwaelder, S.M., and Burridge, K. (1999). Bidirectional signaling between the cytoskeleton and integrins. Curr. Opin. Cell Biol. *11*, 274–286.
6. Furuta, Y., Ilic, D., Kanazawa, S., Takeda, N., Yamamoto, T., and Aizawa, S. (1995). Mesodermal defect in late phase of gastrulation by a targeted mutation of focal adhesion kinase, FAK. Oncogene *11*, 1989–1995.
7. Zervas, C.G., Gregory, S.L., and Brown, N.H. (2001). *Drosophila* integrin-linked kinase is required at sites of integrin adhesion to link the cytoskeleton to the plasma membrane. J. Cell Biol. *152*, 1007–1018.
8. Su, Y.C., Han, J., Xu, S., Cobb, M., and Skolnik, E.Y. (1997). NIK is a new Ste20-related kinase that binds NCK and MEKK1 and activates the SAPK/JNK cascade via a conserved regulatory domain. EMBO J. *16*, 1279–1290.
9. Ruan, W., Pang, P., and Rao, Y. (1999). The SH2/SH3 adaptor protein dock interacts with the Ste20-like kinase misshapen in controlling growth cone motility. Neuron *24*, 595–605.
10. Kyriakis, J.M. (1999). Signaling by the germinal center kinase family of protein kinases. J. Biol. Chem. *274*, 5259–5262.
11. Dan, I., Watanabe, N.M., and Kusumi, A. (2001). The Ste20 group kinases as regulators of MAP kinase cascades. Trends Cell Biol. *11*, 220–230.
12. Treisman, J.E., Ito, N., and Rubin, G.M. (1997). *misshapen* encodes a protein kinase involved in cell shape control in *Drosophila*. Gene *186*, 119–125.
13. Su, Y.C., Treisman, J.E., and Skolnik, E.Y. (1998). The *Drosophila* Ste20-related kinase misshapen is required for embryonic dorsal closure and acts through a JNK MAPK module on an evolutionarily conserved signaling pathway. Genes Dev. *12*, 2371–2380.
14. Su, Y.C., Maurel-Zaffran, C., Treisman, J.E., and Skolnik, E.Y. (2000). The Ste20 kinase misshapen regulates both photoreceptor axon targeting and dorsal closure, acting downstream of distinct signals. Mol. Cell. Biol. *20*, 4736–4744.
15. Schultz, J., Milpetz, F., Bork, P., and Ponting, C.P. (1998). SMART, a simple modular architecture research tool: identification of signaling domains. Proc. Natl. Acad. Sci. USA *95*, 5857–5864.
16. Georges-Labouesse, E., Mark, M., Messaddeq, N., and Gans-

muller, A. (1998). Essential role of alpha 6 integrins in cortical and retinal lamination. Curr. Biol. *8*, 983–986.
17. Gettner, S.N., Kenyon, C., and Reichardt, L.F. (1995). Characterization of beta pat-3 heterodimers, a family of essential integrin receptors in *C. elegans*. J. Cell Biol. *129*, 1127–1141.
18. Baum, P.D., and Garriga, G. (1997). Neuronal migrations and axon fasciculation are disrupted in *ina-1* integrin mutants. Neuron *19*, 51–62.
19. Hutter, H., Vogel, B.E., Plenefisch, J.D., Norris, C.R., Proenca, R.B., Spieth, J., Guo, C., Mastwal, S., Zhu, X., Scheel, J., et al. (2000). Conservation and novelty in the evolution of cell adhesion and extracellular matrix genes. Science *287*, 989–994.
20. Williams, B.D., and Waterston, R.H. (1994). Genes critical for muscle development and function in *Caenorhabditis elegans* identified through lethal mutations. J. Cell Biol. *124*, 475–490.
21. Fire, A., Xu, S., Montgomery, M.K., Kostas, S.A., Driver, S.E., and Mello, C.C. (1998). Potent and specific genetic interference by double-stranded RNA in *Caenorhabditis elegans*. Nature *391*, 806–811.
22. Bosher, J.M., and Labouesse, M. (2000). RNA interference: genetic wand and genetic watchdog. Nat. Cell Biol. *2*, E31–36.
23. Forrester, W.C., and Garriga, G. (1997). Genes necessary for *C. elegans* cell and growth cone migrations. Development *124*, 1831–1843.
24. McIntire, S.L., Reimer, R.J., Schuske, K., Edwards, R.H., and Jorgensen, E.M. (1997). Identification and characterization of the vesicular GABA transporter. Nature *389*, 870–876.
25. Knobel, K.M., Jorgensen, E.M., and Bastiani, M.J. (1999). Growth cones stall and collapse during axon outgrowth in *Caenorhabditis elegans*. Development *126*, 4489–4498.
26. Tabara, H., Sarkissian, M., Kelly, W.G., Fleenor, J., Grishok, A., Timmons, L., Fire, A., and Mello, C.C. (1999). The *rde-1* gene, RNA interference, and transposon silencing in *C. elegans*. Cell *99*, 123–132.
27. Song, H., and Poo, M. (2001). The cell biology of neuronal navigation. Nat. Cell Biol. *3*, E81–88.
28. Lundquist, E.A., Reddien, P.W., Hartwieg, E., Horvitz, H.R., and Bargmann, C.I. (2001). Three *C. elegans* Rac proteins and several alternative Rac regulators control axon guidance, cell migration and apoptotic cell phagocytosis. Development *128*, 4475–4488.
29. Ishii, N., Wadsworth, W.G., Stern, B.D., Culotti, J.G., and Hedgecock, E.M. (1992). UNC-6, a laminin-related protein, guides cell and pioneer axon migrations in *C. elegans*. Neuron *9*, 873–881.
30. Bateman, J., Reddy, R.S., Saito, H., and Van Vactor, D. (2001). The receptor tyrosine phosphatase Dlar and integrins organize actin filaments in the *Drosophila* follicular epithelium. Curr. Biol. *11*, 1317–1327.
31. Hoang, B., and Chiba, A. (1998). Genetic analysis on the role of integrin during axon guidance in *Drosophila*. J. Neurosci. *18*, 7847–7855.
32. Leung-Hagesteijn, C., Spence, A.M., Stern, B.D., Zhou, Y., Su, M.W., Hedgecock, E.M., and Culotti, J.G. (1992). UNC-5, a transmembrane protein with immunoglobulin and thrombospondin type 1 domains, guides cell and pioneer axon migrations in *C. elegans*. Cell *71*, 289–299.
33. Lundquist, E.A., Herman, R.K., Shaw, J.E., and Bargmann, C.I. (1998). UNC-115, a conserved protein with predicted LIM and actin-binding domains, mediates axon guidance in *C. elegans*. Neuron *21*, 385–392.
34. Steven, R., Kubiseski, T.J., Zheng, H., Kulkarni, S., Mancillas, J., Ruiz Morales, A., Hogue, C.W., Pawson, T., and Culotti, J. (1998). UNC-73 activates the Rac GTPase and is required for cell and growth cone migrations in *C. elegans*. Cell *92*, 785–795.
35. Noselli, S., and Agnes, F. (1999). Roles of the JNK signaling pathway in *Drosophila* morphogenesis. Curr. Opin. Genet. Dev. *9*, 466–472.
36. Xue, Y., Wang, X., Li, Z., Gotoh, N., Chapman, D., and Skolnik, E.Y. (2001). Mesodermal patterning defect in mice lacking the Ste20 NCK interacting kinase (NIK). Development *128*, 1559–1572.
37. Tirode, F., Malaguti, C., Romero, F., Attar, R., Camonis, J., and Egly, J.M. (1997). A conditionally expressed third partner stabilizes or prevents the formation of a transcriptional activator in a three-hybrid system. J. Biol. Chem. *272*, 22995–22999.
38. Retta, S.F., Balzac, F., Ferraris, P., Belkin, A.M., Fassler, R., Humphries, M.J., De Leo, G., Silengo, L., and Tarone, G. (1998). beta1-integrin cytoplasmic subdomains involved in dominant negative function. Mol. Biol. Cell *9*, 715–731.
39. Jin, Y., Jorgensen, E., Hartwieg, E., and Horvitz, H.R. (1999). The *Caenorhabditis elegans* gene *unc-25* encodes glutamic acid decarboxylase and is required for synaptic transmission but not synaptic development. J. Neurosci. *19*, 539–548.
40. Chalfie, M., Tu, Y., Euskirchen, G., Ward, W.W., and Prasher, D.C. (1994). Green fluorescent protein as a marker for gene expression. Science *263*, 802–805.
41. Fire, A., Harrison, S.W., and Dixon, D. (1990). A modular set of *lacZ* fusion vectors for studying gene expression in *Caenorhabditis elegans*. Gene *93*, 189–198.